12th International Conference on Fracture Mechanics of Concrete and Concrete Structures
FraMCoS-12
B.L.A. Pichler, Ch. Hellmich, P. Preinstorfer (Eds)

https://doi.org/10.21012/FC12.1205
MS15-1:1

EXPERIMENTAL STUDY ON CRACK DISTRIBUTION OF RC MEMBERS WITH REINFORCING BARS COATED WITH FIBER REINFORCED CEMENTITIOUS COMPOSITES

BOCHAO SONG[*], NAOSHI UEDA[*]

[*] Kansai University
3-3-35, Yamate-cho, Suita, Osaka, Japan
e-mail: k979406@kansai-u.ac.jp

Key words: Fiber Reinforced Concrete, Composites, RC beam, Flexural load test Crack distribution, DIC

Abstract: A reinforcing bar coated with Fiber Reinforced Cementitious Composites (FRCC), called "coated rebar," has possibilities of enhancing not only tensile properties but also resistance to rebar corrosion when embedded in concrete members. This study aims to investigate the bond behavior of coated rebars used in RC members. Several FRCC with different strength and ductility, including Ultra High Performance-Strain Hardening Cementitious Composite (UHP-SHCC), were used as the coating materials. Tensile tests for the coated rebars were conducted to evaluate the crack distributions of the coated bars themselves. Flexural load tests were also performed to evaluate the influences of coated rebars on crack distribution in RC beams. As a result, the experimental results demonstrated that the crack distribution of RC beams depends on the cracking ability of the coated rebar. The coated rebar with UHP-SHCC, having excellent cracking ability, shows better crack distribution in the RC beam than those with the other materials in this study.

1 INTRODUCTION

It is well known that in earthquake-prone countries, unexpected large earthquakes often lead to the collapse of RC columns, causing significant structural damage and resulting in substantial loss of life and economic impact. Therefore, in the seismic design of RC structures, columns need to be designed with sufficient flexural deformation capacity to ensure energy absorption under large earthquakes.

In a typical failure mode of RC columns, longitudinal bars tend to buckle under cyclic loadings, leading to a rapid decrease in load-bearing capacity and resulting in a collapse [1-3]. Therefore, to improve the deformation capacity of RC columns, it is crucial to prevent buckling effectively.

In recent years, Nakamura et al. [4] has proposed a new buckling mechanism for longitudinal rebars. The mechanism is that horizontal internal cracks first initiate from the longitudinal rebars, reducing the constraint provided by the concrete cover, and resulting to the buckling of rebars. Based on this mechanism, the authors [5] proposed a new method to prevent rebar buckling using coated rebars, specifically rebars coated with Ultra High Performance-Strain Hardening Cementitious Composite (UHP-SHCC) [6]. This method can suppress the initiation of horizontal cracks by the longitudinal rebars due to the high strength and ductility characteristics of UHP-SHCC, thereby preventing buckling. Its effectiveness has been validated experimentally, however, the crack patterns in RC members with coated bar changed. These crack patterns could be

influenced by the tensile cracking capacity of the coating material and the bond behaviour between the coated rebars and the surrounding concrete.

This study aims to investigate the effects of the coated rebar on the flexural crack distribution of concrete members under bending moments. Specifically, the surface shapes and used materials of the coated rebar changed and their impacts on the bond behaviour between the coated rebar and the concrete were investigated. Adding to the UHP-SHCC, Ultra High Performance Concrete (UHPC) and Strain Hardening Cementitious Composite (SHCC) were used as the coating materials. The cracking capacity of each coated rebar was evaluated by a direct tensile test, and its impact on RC members was investigated through a flexural load test. To clarify the details of crack initiation, Digital Image Correlation (DIC) was applied in these experiments.

2 EXPERIMENTAL PROGRAMS

2.1 Material Used

In this study, three materials with distinct properties, UHP-SHCC, UHPC, and SHCC were used to clearly compare their different cracking behavior effects on crack distribution in coated rebar, as well as the mechanical performance and flexural crack distribution of RC members. In each material, different short fibers, PE fibers, steel fibers, and PVA fibers, were mixed in UHP-SHCC, UHPC, and SHCC, respectively. Their details are shown in Table 1.

Table 1: Details of the fibers

	Density (g/cm^3)	Tensile strength (MPa)	Elastic modulus (GPa)	Diameter (μm)	Length (mm)
PE	0.97	2700	88	12	6
PVA	1.3	1200	28	40	12
SF	7.85	2000	210	200	13

The properties of each material are summarized in Table 2.

The tensile stress-strain relationships of each coating material are shown in Figure 1. These results were obtained from the uniaxial tensile tests for three dumbbell shaped specimens, and the average strain was obtained from the elongation in 100 mm length of the specimen. Notably, the two UHP-SHCC in the figure, UHP-SHCC1 and UHP-SHCC2, differ only in their cast batches. For UHP-SHCC2, one specimen failed outside the measurement range, leaving only two samples. The two batches of UHP-SHCC showed no significant differences in tensile strength and elongation capacity, both approximately exceeding 4.0 N/mm² and 2.0%, respectively, while UHPC demonstrated 6.0 N/mm² and 0.15%, and SHCC exhibited 1.5 N/mm² and 1.0%.

Table 2:-Material property

Material	Tensile strength (MPa)	Compressive strength (MPa)
UHP-SHCC1	6.1	90.5
UHP-SHCC2	5.0	93.0
UHPC	6.1	108.4
SHCC	1.5	30.3

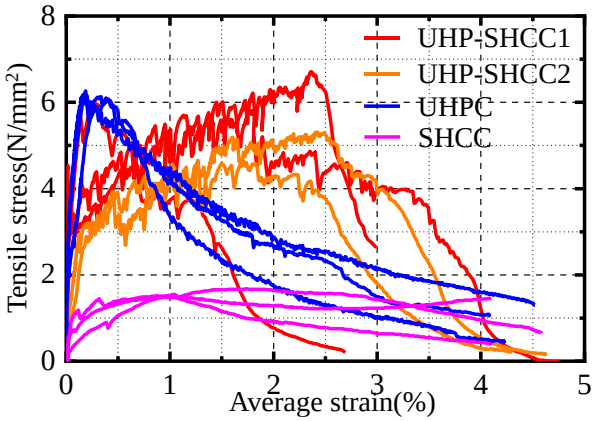

Figure 1: Tensile stress-strain relationships.

The compressive strengths of the coating materials were determined. The results represent the mean values of three cylindrical specimens, each with diameters of 50 mm and heights of 100 mm. The compressive strength of UHP-SHCC1 and UHP-SHCC2 were 90.5 and 93.0 MPa, respectively. In comparison, UHPC exhibited a slightly higher value of 108 MPa, whereas SHCC had a relatively low compressive strength of 30.3MPa.

For the steel bars used in this study, the nominal yield strength was 384 MPa.

2.2 Tensile test

Four different types of coated rebars were designed for tensile tests. Table 3 lists the specimen's details. The outline of the specimen details is shown in Figure 2. The coating length of the specimens was 500 mm, with the thickness of the coating, excluding the rib thickness, being 10 mm by using Polyethylene tubes. The specimens, D-US, D-U, and D-S had ribs with a height of 5 mm and a spacing of 10 mm, while R-US had smooth surface to investigate the influence of surface on the bond behavior. Note that unbonded regions of 50 mm in length were set at both side of the coating area. All specimens were fabricated by placing the rebar in the center of a tube and injecting mortar into the tube. After the mortar hardened, the tube was removed and cured under wetted clothes and plastic sheets.

All specimens were subjected to axial tensile loading using an Amsler universal testing machine. Displacements within the central 400 mm of the specimens were measured using Pi-shape gauges, each with a gauge length of 50 mm and a capacity of ±5 mm. The loading was paused at around 8 mm of total displacement of the gauges to record the crack pattern in the specimens. Loading was then resumed until the one of the gauges reached their maximum capacity, followed by the unloading.

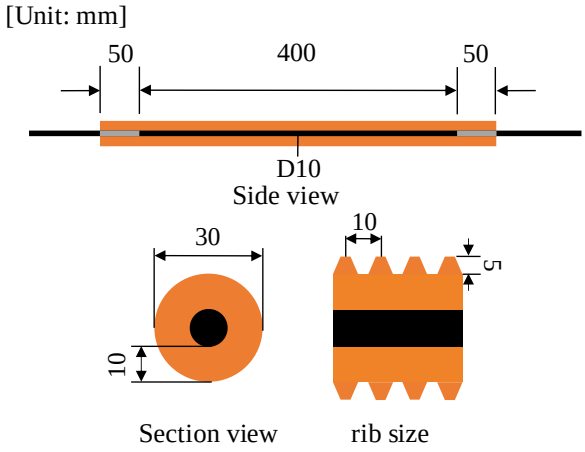

Figure 2: Configuration of the specimens.

2.3 Flexural load test

The RC beams were used for the flexural load tests. The section dimensions were 100 mm in width and 200 mm in height. One rebars with a diameter of 10 mm were arranged at 165 mm in effective depth and a reinforcement ratio of 0.47%. Stirrups of 10 mm in diameter were also arranged to prevent the diagonal cracks in both shear spans.

Five specimens with several types of coated rebars listed in Table 3 were prepared including one control specimen, NC. Note that RB-US indicates that the epoxy resin was applied as an adhesion on the smooth surface of R-US in order to enhance the bond chemically.

For the specimens with coated rebar, the coating length was 1100 mm from the center of the beam, extending 100 mm over each loading point. Unlike the specimen of the tensile test, the RC beams have no unbonded region.

The loading condition was four-point bending method. The loading system consisted

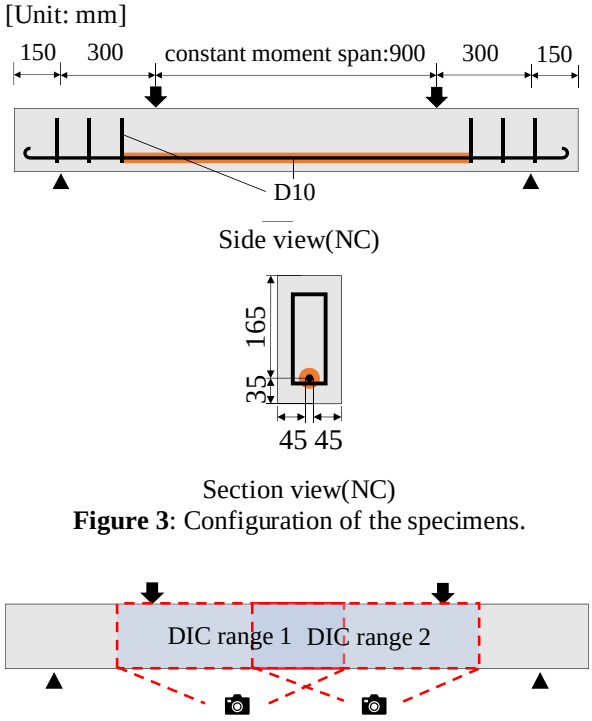

Figure 3: Configuration of the specimens.

Figure 4: DIC range.

of a hydraulic jack, with manual control of the loading rate. Five LVDT, each with a capacity of 25 mm, were installed to measure displacement in equivalent moment span including both loading points as shown in Figure 3. Additionally, Digital Image Correlation (DIC) was employed, with two cameras set up to monitor crack progression in each specimen, as shown in Figure 4.

The compressive strengths of the concrete were 37.2 MPa for the R-US Specimen and NC Specimen, 38.4MPa for D-US Specimen and RB-US, and 38.3MPa for the D-U Specimen and D-S Specimen.

Table 3: Details of specimens

	Coating material	Surface condition
NC	-	-
R-US	UHP-SHCC1	round
RB-US*	UHP-SHCC2	round
D-US		deformed
D-U	UHPC	
D-S	SHCC	

*Epoxy resin was applied on the surface of coated rebar

3 TENSILE TEST RESULTS AND DISCUSSION

3.1 Crack distribution of coated rebar

Figure 5(a) and 5(b) illustrates examples of the crack patterns observed in the specimens after testing, with cracks highlighted in red for clarity. For the R-US specimen, a large number of microcracks developed throughout the specimen, and one or two cracks widened significantly and localized in the end. A similar crack pattern was observed in the D-US specimen, however, the cracks tended to exhibit at the necked parts and rarely appeared on the ribs. Multiple cracks in the D-U specimen, whereas relatively few cracks appeared in the D-S specimen, respectively.

R-US

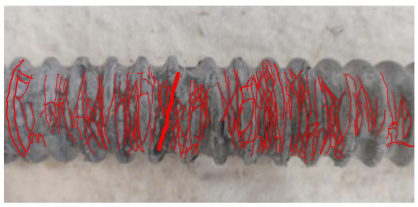

D-US

Figure 5(a): Crack distribution.

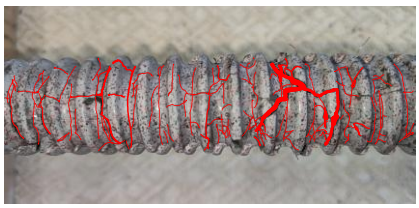

D-U

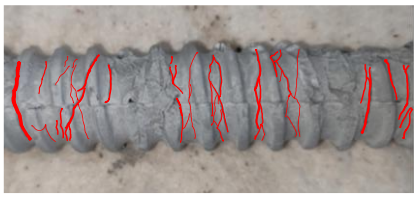

D-S

Figure 5(b): Crack distribution.

3.2 Average crack spacing and crack width

Figure 6 show the average crack spacing, and the average crack width at the 8 mm of total displacement. These values were calculated based on the displacements measured by each gauge and the crack count determined by visual inspection within the measurement range.

For the R-US and D-US specimens, both the average crack width and crack spacing are

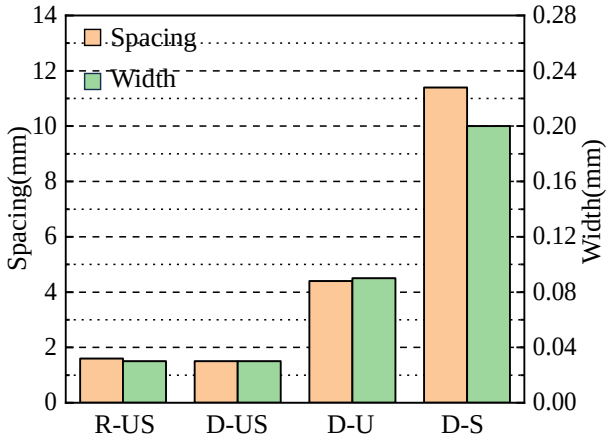

Figure 6: Crack spacing and width.

almost the same: 1.6 mm and 0.03 mm for the R-US specimen, and 1.5 mm and 0.03 mm for the D-US specimen, respectively. Regarding the influence of surface geometry, these results indicate that the presence of ribs does not significantly influence the crack distribution capability.

On the other hand, those values are 4.4 mm and 0.09 mm for the D-U specimen, and 11.4 mm and 0.2 mm for the D-S specimen, respectively. Regarding the difference of covering materials, there results clarified that the D-US specimen generated a larger number of narrower cracks. This behavior is attributed to the strain-hardening properties of UHP-SHCC, which allow for sustained multiple cracking even at higher deformation levels. In contrast, UHPC, with its strain-softening characteristics, loses its ability to generate further cracks at relatively small deformation levels. Similarly, the reason why the D-S specimen exhibited the fewest cracks and the widest crack widths is that SHCC has lower tensile strength despite its deformation capacity compared to UHP-SHCC and UHPC. This results in fewer cracks, with existing ones widening further.

4 FLEXURAL LOAD TEST

4.1 Load-deflection relationships

Figure 7(a) shows the load-deflection relationships for D-US, R-US, and RB-US specimens, while Figure 7(b) shows those of D-US, D-U, and D-S specimens. The former indicates the influence of the surface geometry of the coated bars, while the latter indicates the influence of material properties of the coated materials. The result of the NC specimen is also presented for the comparison. All specimens failed in flexural yield with large deflection beyond 80 mm as shown in Table 4. As mentioned in Chapter 1, this research focuses on the influence of coated materials on the flexural crack distribution in RC members. Since the initiation and propagation of flexural cracks mainly occur before rebar yielding, this chapter only discusses the flexural behavior up to a 10 mm deflection.

Table 4: Summary of the test results.

	Deflection (mm)	Initial cracking load (kN)	Post cracking flexural stiffness (kN/mm)
NC	109	16.5	4.6
R-US	100	16.1	4.7
D-US	105	16.8	4.2
RB-US	100	16.2	4.1
D-U	109	18.1	4.5
D-S	83.6	13.7	4.9

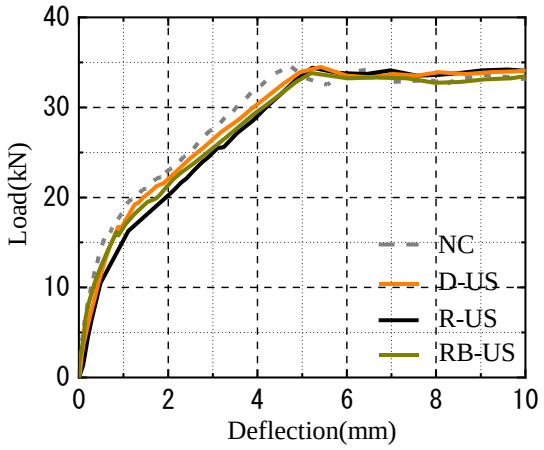

Figure 7(a): Load-deflection relationships.

Focusing on the flexural cracking points, all specimens except the R-US specimen exhibited lower load compared to the NC specimen, as shown in Table 4. Because the concrete strength varies to some extent and influences the flexural cracking load, and reinforcement has less influence on it, those differences are understood to come from any variations throughout the experiment.

Generally, the bond between concrete and rebars influences the slope of the load-deflection relationship after the flexural cracking. Therefore, the slope, referred to as post-cracking flexural stiffness, was calculated for each specimen. Note that in this study, the stiffness was calculated based on the least square method between the flexural cracking point and the yielding point. The results are summarized in Table 4.

The NC specimens, the post-cracking flexural stiffness was 4.6 kN/mm. In comparison, for the R-US specimens was 4.7 kN/mm with no significant difference.

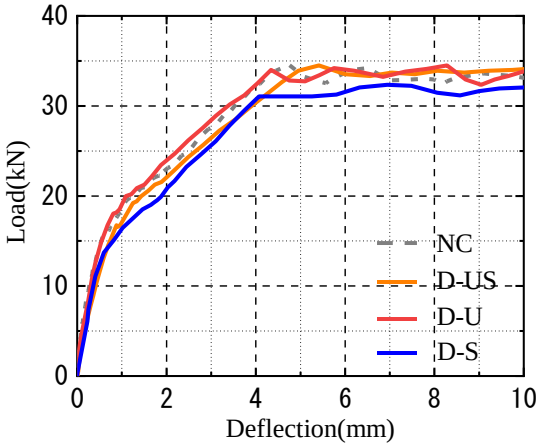

Figure 7(b): Load-deflection relationships.

However, the D-US and RB-US specimens demonstrated slightly lower stiffness, at 4.2 kN/mm and 4.1 kN/mm, respectively.

On the other hand, focusing on the influence of coated materials, the post-cracking flexural stiffness of D-U specimens was 4.5 kN/mm, and for D-S specimens was 4.9 kN/mm, both showed difference with D-US specimens, but similar with the NC specimen. Since the surface geometries of the three specimens were identical, their behaviors were thought to depend on the material properties. However, considering the overall behavior of the three beams, the differences can be attributed to variations in the experimental conditions.

These results suggest that the rib or the application of epoxy resin on the surface, as well as the tensile material properties of the coated materials, had no significant impact on the post-cracking stiffness of the specimens.

4.2 Crack distribution by DIC

For the specimens described in the previous section, the surface crack distribution at yield of the specimens was confirmed using DIC. Figure 8 shows the distribution of maximum principal strain between the constant moment span. In the images, the blue-purple regions represent areas with extremely small strain, and strain increases as the color changes to yellow-green, yellow, and red. Additionally, to facilitate the observation and comparison of the overall cracking behavior of the specimen, the overlapping sections of the left and right sides captured at the same moment were overlapped and stitched together.

Focusing on the number of cracks, In each image, the number of cracks has been labeled. It is worth noting that cracks located directly beneath the loading points were excluded.

The R-US specimen exhibited fewer cracks compared to the NC specimen, while the D-US and RB-US specimens showed no significant difference. On the other hand, the D-U

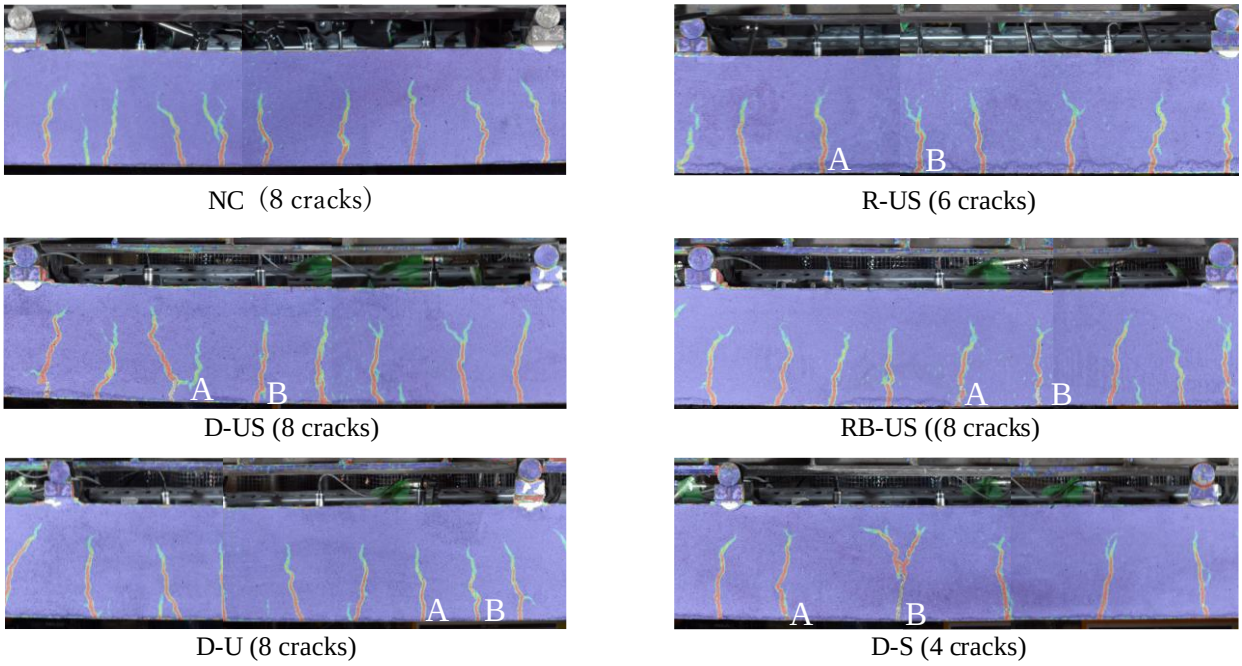

NC（8 cracks）　R-US (6 cracks)

D-US (8 cracks)　RB-US ((8 cracks)

D-U (8 cracks)　D-S (4 cracks)

Figure 8: Crack distribution.

specimen showed no notable difference compared to the D-US specimen, whereas the D-S specimen exhibited significantly fewer cracks. Specifically, the D-S specimen has wider cracks compared to the others, and one of these cracks exceeds the measurement range, resulting in no color display. This suggested that the lower yield load of the D-S specimen, as observed in the load-deflection relationship, resulted from localized stress concentration.

Normally, the bond between rebar and concrete influence the crack spacing in RC member, with stronger bond conditions leading to smaller crack spacing. To evaluate the crack distribution quantitatively, the average crack spacing at the yield load was measured using image analysis software, ImageJ, to analyze the aforementioned images. Note that, due to image quality issues, the measurement results have an error margin of approximately 3 mm.

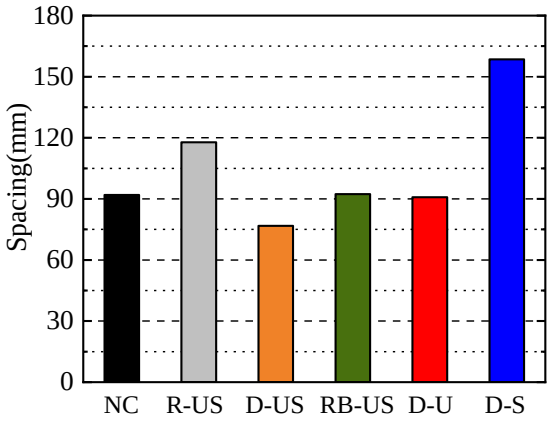

Figure 9: Crack spacing.

The crack spacing of each specimen are shown in Figure 9. For the NC specimen, crack spacing was 91.9 mm. For the specimens with the coated rebars, for the R-US specimen, which has no rib on the surface, it was 118 mm, whereas for the D-US and RB-US specimens, they were 76.8 mm and 92.3 mm, respectively. This indicates that, compared to the NC specimen, the bond between the coated rebars and the concrete layer in the R-US specimen is weaker. In contrast, the D-US specimen exhibits a stronger bond provided by the mechanical interlocking of ribs, which surpasses the chemical adhesion observed in the RB-US specimen.

On the other hand, compared the different coated materials, for the D-U specimen, the crack spacing was 90.8 mm, which was wider than that of the D-US specimen. The D-S specimen exhibited the largest crack spacing at 159 mm. Despite their identical surface geometries, significant differences in crack spacing were observed among the specimens. These differences showed a consistent tendency corresponding to the variations in the cracking capacity of the coated rebar itself.

4.3 Internal crack

To investigate the cracking mechanisms for the coated mortars and concrete, internal crack distributions were observed by cutting the beam specimen after the flexural test. Figure 10 shows a schematic of the internal crack observations of the beam specimens, which were cut along the constant moment span.

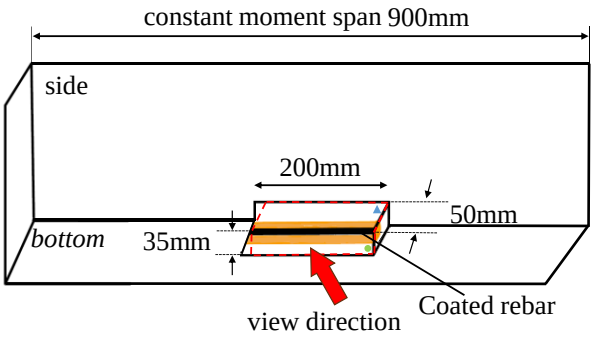

Figure 10: Cutting schematic.

Figures 11(a) and 11(b) present the unfolded view of the cut regions shown in Figure (10), illustrating the internal crack of each specimen. Notably, for comparison, the internal crack of the D-US specimen are included in both sets of figures. The triangles and circles marked in the figures correspond to the same spatial positions as the respective markers in Figure (10) before unfolding. These diagrams were sketched based on the photographs; therefore, the crack wide does not completely reflect the actual conditions. The top and bottom of each diagram connected to the side surface and bottom surface of the specimen, respectively. Cracks labeled as A and B are corresponded to the same markings

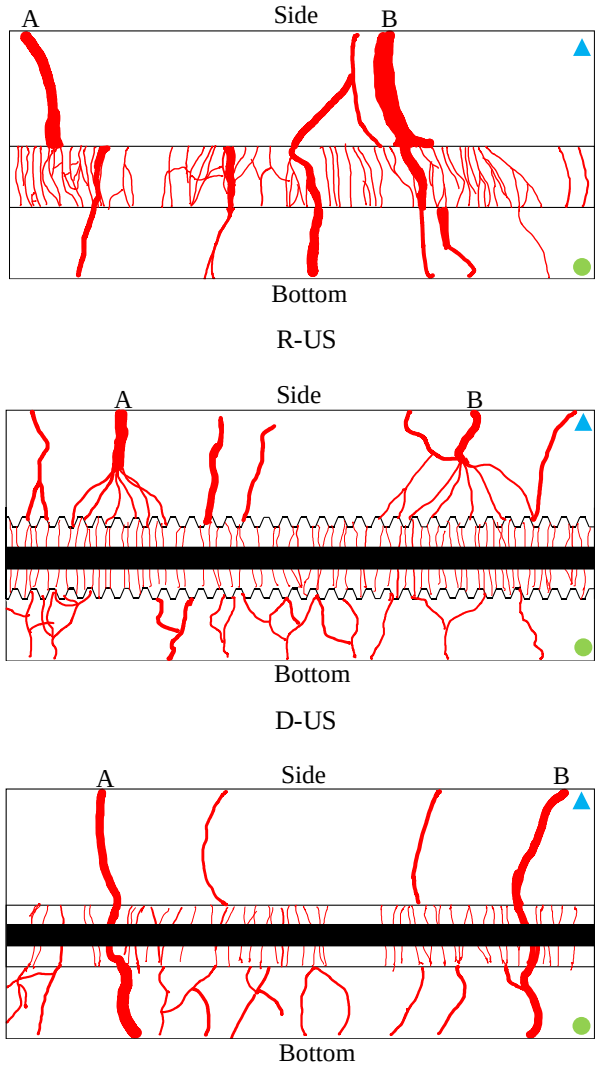

Figure 11(a): Internal crack.

in the DIC images. Note that, only the R-US specimen, as the coating layer was not fully cut through, the cracks shown in the figure represent those observed on the surface of the coated rebar.

For all specimens, the coated rebars exhibited a large number of cracks compared to the concrete cover. In RC beams, the cracking process generally begins with the development of a flexural crack at the bottom of the beam. This is followed by the rebar working once the crack reaches it. Therefore, the crack distribution in coated rebars is thought to occur due to the tensile state between the flexural cracks of concrete.

From this perspective, in the R-US and RB-US specimens, where there are no ribs on the coated rebars, the cracks in the coated rebars were localized near the flexural cracks in the concrete cover, which had wider crack width. In the R-US specimen, other localized cracks were observed apart from flexural cracks, whereas no other localization was observed in the RB-US specimen. Both specimens formed small cracks in the concrete cover, but the R-US specimen had fewer cracks compare to the RB-US specimen. In contrast to the R-US and RB-US specimens, the D-US specimen exhibited a different crack pattern. Cracks in the concrete cover even dispersed to several fine cracks near coated bars, reaching to the rib. No localized cracks observed in the coated rebars in the D-US specimen.

As mentioned before, the bond of coated rebar starts to work once the flexural cracks reach it. In the R-US specimen, slippage occurred due to its smooth geometry, and only the weak friction between the coated rebar and the concrete was acting. The coated rebar resisted the tensile force without transmitting it to the surrounding concrete, resulting in fine cracks in the coated rebar and wider cracks in the cover concrete. Meanwhile, in the RB-US specimen, where the bond is attributed to the chemical adhesion, slightly stronger tensile forces were transmitted to the surrounding concrete compared to the R-US specimen. This resulted in fewer fine cracks in the coated rebar and more cracks in the cover concrete.

In contrast, in the D-US specimen, the ribs on the surface of coated rebar could transmit large tensile forces to the surrounding concrete, creating a strongly bond. Several fine cracks near the ribs of the covered rebars, even causing the flexural cracks to separate nearby. This suggests that the bond conditions of the D-US specimen could be different from what is commonly understood, which refers to the tensile conditions at both ends as described before.

On the other hand, for specimens using different coating materials, the D-U and D-S specimen, the cracks in the coated rebars localized to those in the cover concrete and developed fewer cracks compared to the D-US specimen. The cracks in the D-S specimen were highly concentrated than those in the D-U specimen. In the cover concrete between the

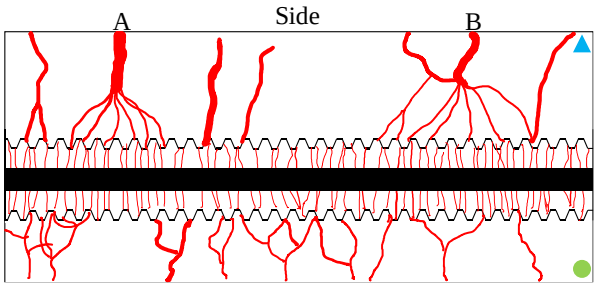

D-US (same as Figure11(a))

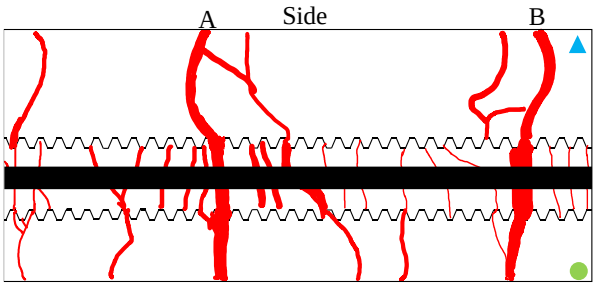

D-U

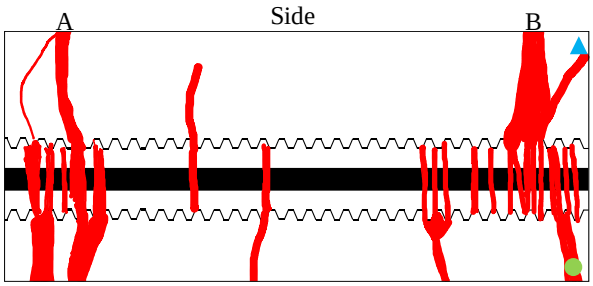

D-S

Figure 11(b): Internal crack.

flexural cracks, the D-U specimen exhibited a small number of small cracks connected to the ribs, whereas the D-S specimen produced almost no small cracks.

Even though their coated rebars have the same surface geometry as the D-US specimen, the flexural cracks reached the coated rebars without separating into fine cracks as observed in the D-US specimens. This suggested that the bond of the D-U and D-S specimen were weaker than that of D-US. As mentioned in the previous chapter, UHPC and SHCC have a weaker cracking capacity under tensile conditions compared to UHP-SHCC. The results of internal cracks suggest that, compared to UHP-SHCC, UHPC and SHCC in flexural crack regions lose tensile capacity earlier, resulting in a loss of force transmission from coated rebar to concrete and widening of existing cracks.

Moreover, the situation between the flexural cracks in the D-S specimen might be more complex. Considering that the D-S specimen exhibited significantly lower yield strength under the flexural load tests while showing no significant difference in the tensile tests compared to other specimens, the cracking behavior between flexural cracks could also be attributed to SHCC's lower compressive strength. This lower strength, which is weaker than that of concrete, leads to the damage of the rib of coated rebar. This could prevent the coated rebar from transmitting sufficient tensile force to the cover concrete, leading to relative slippage between the coated rebar and the surrounding concrete, resulting in fewer cracks in the concrete. However, as visible signs of rib damage or separation between the coated rebar and the concrete cover were not clearly observed at a macroscopic level during this experiment, further experimental verification is necessary.

5 CONCLUSIONS

In this study, for the reinforcement method "coated rebar", the effects of coated materials and surface conditions on crack distribution of the coated rebar itself under uniaxial tensile conditions were clarified. Additionally, their bond characteristics between concrete was investigated from the perspective of the flexural stiffness and crack distribution of RC beams. Based on the studies above, the following conclusions are drawn:

1.The crack distribution capability of coated rebar under uniaxial tensile conditions is related to the mechanical performance of the coated materials under tensile stress. In this study, coated rebar using UHP-SHCC exhibited the best crack distribution capability compared to UHPC and SHCC.

2.The surface condition of the coated rebar or the tensile material properties of coated material did not significantly affect the flexural stiffness after cracking of RC beams.

3.The spacing of flexural cracks in beams was influenced by the surface condition of the coated rebar and the mechanical properties of the coated material. Compared to round surfaces, ribs or epoxy-coated surfaces resulted in smaller crack spacing, indicating that they enhanced the bond between the coated rebar and the concrete.

4. Among different coated materials, a high bond was evaluated when using UHP-SHCC than SHCC or UHPC from the crack distributions, especially, the internal cracks. The bond mechanisms between concrete and the coated rebar with UHP-SHCC might differ from the conventional ones. Internal cracks disperse finely, and no primary cracks were observed near the coated rebars.

REFERRENCES

[1] Scribner, C. F.: Reinforcement Buckling in Reinforced Concrete Flexural Members, ACI Journal, Vol.83, Issue 6, pp.966-973, 1986.

[2] R.P. Dhakal, K. Maekawa. Reinforcement stability and fracture of cover concrete in reinforced concrete members. J Struct Eng, 128 (10) (2002), p. 1253

[3] Hoshikuma, J., Unjoh, S. and Shiojima, A.: Effect of Cov-er Concrete on Anti-Buckling of Longitudinal Bars in Re-inforced Concrete Columns, Structural engineer-ing/Earthquake Engineering, Vol.23, No.1, pp.101s-108s, 2006.

[4] H. Nakamura, T. Miura, Y. Yamamoto: A new buckling mechanism of longitudinal rebar related to horizontal crack propagation in beam cross section under cyclic loadings, fib congress 2018.

[5] Bochao Song N. Ueda H. Nakamura：Experimental investigation on buckling restrained of RC members with steel bars covered by UHP-SHCC Proceedings of the Japan Concrete Institute Vol. 2 (46) page：997 - 1002 2024.7(in Japanese)

[6] M. Kunieda, E. Denarié, E. Brühwiler, H. Nakamura: Challenges for Strain Hardening Cementitious Composites – Deformability Versus Matrix Density, Proc. of the fifth International RILEM Workshop on HPFRCC, pp.31-38, 2007.